

Suppression of spin-density-wave transition and emergence of ferromagnetic ordering of Eu^{2+} moments in $\text{EuFe}_{2-x}\text{Ni}_x\text{As}_2$

Zhi Ren, Xiao Lin, Qian Tao, Shuai Jiang, Zengwei Zhu, Cao Wang, Guanghan Cao* and Zhu'an Xu†

¹*Department of Physics, Zhejiang University, Hangzhou 310027, China*

We present a systematic study on the physical properties of $\text{EuFe}_{2-x}\text{Ni}_x\text{As}_2$ ($0 \leq x \leq 0.2$) by electrical resistivity, magnetic susceptibility and thermopower measurements. The undoped compound EuFe_2As_2 undergoes a spin-density-wave (SDW) transition associated with Fe moments at 195 K, followed by antiferromagnetic (AFM) ordering of Eu^{2+} moments at 20 K. Ni doping at the Fe site simultaneously suppresses the SDW transition and AFM ordering of Eu^{2+} moments. For $x \geq 0.06$, the magnetic ordering of Eu^{2+} moments evolves from antiferromagnetic to ferromagnetic (FM). The SDW transition is completely suppressed for $x \geq 0.16$, however, no superconducting transition was observed down to 2 K. The possible origins of the AFM-to-FM transition and the absence of superconductivity in $\text{EuFe}_{2-x}\text{Ni}_x\text{As}_2$ system are discussed.

PACS numbers: 75.30.Fv; 75.50.-y; 75.60.Ej

I. INTRODUCTION

The discovery of superconductivity up to 56 K in iron-based arsenides [1, 2, 3, 4, 5, 6, 7] has aroused great interest in the community of condensed matter physics. The undoped parent compounds adopt the tetragonal structure at room temperature, which consists of $[\text{Fe}_2\text{As}_2]^{2-}$ layers separated alternatively by $[\text{Ln}_2\text{O}_2]^{2+}$ [8, 9] or A^{2+} ($A=\text{Ca}, \text{Sr}, \text{Ba}, \text{Eu}$) layers [10, 11, 12, 13]. At low temperatures, the parent compounds undergo a structural phase transition from tetragonal to orthorhombic, accompanied [14] or followed [15] by a SDW-like antiferromagnetic (AFM) phase transition. Doping with electrons or holes in the parent compounds suppresses the phase transitions and induces the high temperature superconductivity. This intimate connection between superconductivity and magnetism suggests unconventional superconductivity in the iron-based arsenides. [16, 17, 18]

Very recently, superconductivity has been observed in $\text{LaFe}_{1-x}\text{M}_x\text{AsO}$ [19, 20, 21] and $\text{BaFe}_{2-x}\text{M}_x\text{As}_2$ [22, 23] ($M=\text{Co}$ and Ni). These findings are quite remarkable and challenge our common wisdom of superconductivity, which shows that direct doping in the superconducting-active blocks generally destroys superconductivity. In high T_c cuprates, actually, Ni substitution for Cu in the CuO_2 planes drastically reduces T_c . Hence these experimental results provide clues to the superconducting mechanism for the iron-based arsenide superconductors. Currently, an itinerant scenario within rigid band model is more favored to understand this unusual doping-induced superconductivity. [24]

EuFe_2As_2 is a unique member in the ternary iron arsenide family due to the fact that Eu^{2+} ions carry local moments, which orders antiferromagnetically below 20 K. [12, 25, 26] Except this AFM transition, the physi-

cal properties of EuFe_2As_2 were found to be quite similar with those of its isostructural compounds BaFe_2As_2 and SrFe_2As_2 , [25] both of which become superconducting upon appropriate doping [27, 28, 29]. It was then expected that EuFe_2As_2 could be tuned superconducting through similar doping strategies. Indeed, superconductivity with T_c over 30 K has been observed in $(\text{Eu}, \text{K})\text{Fe}_2\text{As}_2$ [30] and $(\text{Eu}, \text{Na})\text{Fe}_2\text{As}_2$ [31].

Doping at the Fe site in EuFe_2As_2 takes advantage of inducing possible superconductivity while leaving the magnetic Eu^{2+} layers intact, which could provide us insight to the interplay between superconductivity and magnetism. Here we report a systematic study on the physical properties in $\text{EuFe}_{2-x}\text{Ni}_x\text{As}_2$ ($0 \leq x \leq 0.2$) system. It was found that both the SDW ordering of Fe moments and the AFM ordering of Eu^{2+} moments were suppressed by substituting Fe with Ni. Ferromagnetic (FM) ordering of Eu^{2+} moments emerges for $x \geq 0.06$. While the SDW transition is completely suppressed for $x \geq 0.16$, no superconducting transition was observed down to 2 K in $\text{EuFe}_{2-x}\text{Ni}_x\text{As}_2$, in contrast with the superconductivity in $\text{BaFe}_{2-x}\text{Ni}_x\text{As}_2$ [23]. Our results suggest a strong coupling between the magnetism of Eu^{2+} ions and the conduction electrons of $[\text{Fe}_{2-x}\text{Ni}_x\text{As}_2]^{2-}$ layers.

II. EXPERIMENT

Polycrystalline samples of $\text{EuFe}_{2-x}\text{Ni}_x\text{As}_2$ ($x = 0, 0.03, 0.06, 0.09, 0.12, 0.16$ and 0.2) were synthesized by solid state reaction with EuAs , Fe_2As and Ni_2As . EuAs was presynthesized by reacting Eu grains and As powders in evacuated silica tube at 873 K for 10 h then 1123 K for 36 h. Fe_2As was presynthesized by reacting Fe powders and As powders at 873 K for 10 h and 1173 K for 2.5 h. Ni_2As was presynthesized by reacting Ni powders and As powders at 873 K for 10 h then 1073 K for another 10 h. The powders of EuAs , Fe_2As and Ni_2As were weighed according to the stoichiometric ratio, thoroughly ground and pressed into pellets in an argon-filled glove-box. The

*Electronic address: ghcao@zju.edu.cn

†Electronic address: zhuan@zju.edu.cn

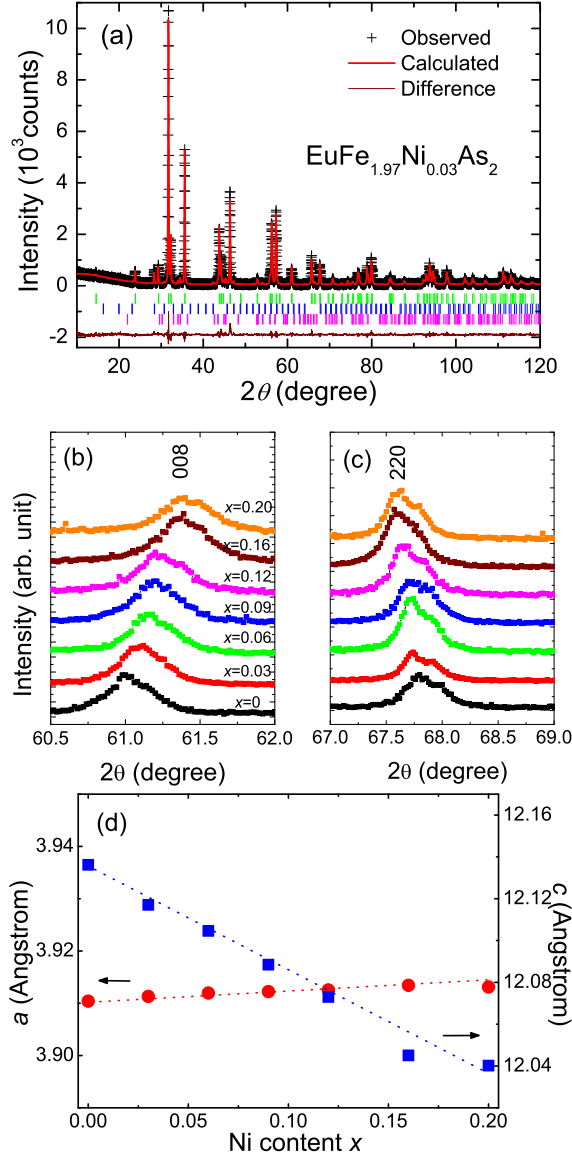


FIG. 1: (Color online) (a) X-ray powder diffraction pattern at room temperature and the Rietveld refinement profile for the $\text{EuFe}_{1.97}\text{Ni}_{0.03}\text{As}_2$ sample. Eu_2O_3 ($\sim 1.4\%$) and $\text{Fe}_{0.985}\text{Ni}_{0.015}\text{As}$ ($\sim 6\%$) are also included in the refinement. (b) and (c) represent the (008) and (220) diffraction peaks for the $\text{EuFe}_{2-x}\text{Ni}_x\text{As}_2$ samples, respectively. (d) Refined lattice parameters plotted as functions of Ni content x .

pellets were sealed in evacuated quartz tubes and annealed at 1173 K for 24 h and furnace-cooled to room temperature. Powder x-ray diffraction (XRD) was performed at room temperature using a D/Max-rA diffractometer with $\text{Cu-K}\alpha$ radiation and a graphite monochromator. The data were collected with a step-scan mode. The structural refinements were performed using the programme RIETAN 2000.[32] The electrical resistivity was measured using a standard four-probe method. The measurements of dc magnetic properties were performed on a

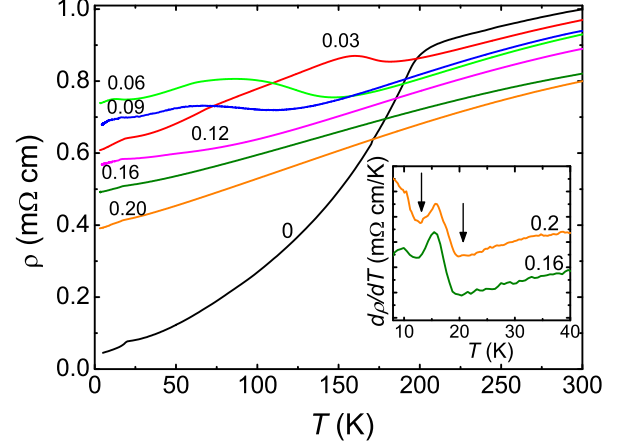


FIG. 2: (Color online) Temperature dependence of resistivity for the $\text{EuFe}_{2-x}\text{Ni}_x\text{As}_2$ samples. The inset shows derivative plots for $x=0.16$ and 0.2 below 40 K. The anomalies are marked by arrows.

Quantum Design Magnetic Property Measurement System (MOMS-5). Thermopower measurements were carried out in a cryogenic refrigerator down to 17 K by a steady-state technique with a temperature gradient ~ 1 K/cm.

III. RESULTS AND DISCUSSION

The crystal structure for all the $\text{EuFe}_{2-x}\text{Ni}_x\text{As}_2$ ($x = 0, 0.03, 0.06, 0.09, 0.12, 0.16, 0.2$) samples at room temperature were refined with the tetragonal ThCr_2Si_2 structure. An example of the refinement profile for $\text{EuFe}_{1.97}\text{Ni}_{0.03}\text{As}_2$ is shown in Fig. 1(a). The weighted pattern factor and goodness of fit are $R_{wp} \sim 11.2\%$ and $S \sim 1.6$, indicating a fairly good refinement. Minor impurity phases of Eu_2O_3 and $\text{Fe}_{0.985}\text{Ni}_{0.015}\text{As}$ are also identified. In addition, the refined occupancies are close to the nominal value. With increasing Ni content, the (008) diffraction peaks shift towards higher angles (Fig. 1(b)) while the (220) diffraction peak shift towards lower angles (Fig. 1(c)). This observation is consistent with the result from the Rietveld refinements, which show that a -axis increases slightly while c -axis shrinks remarkably with increasing Ni content, as shown in Fig. 1(d).

Figure 2 shows the temperature dependence of normalized resistivity (ρ) for the $\text{EuFe}_{2-x}\text{Ni}_x\text{As}_2$ samples. The ρ value at 300 K decreases with increasing Ni content, which is probably attributed to the increase of carrier concentration induced by the Ni doping. For the parent compound, ρ drops rapidly below 195 K and shows a kink at ~ 20 K. The former is associated with a SDW transition of Fe moments while the latter is due to the AFM ordering of Eu^{2+} moments.[25] On Ni doping, the anomaly in ρ associated with the SDW transition is presented as an upturn, followed by a hump. This behavior

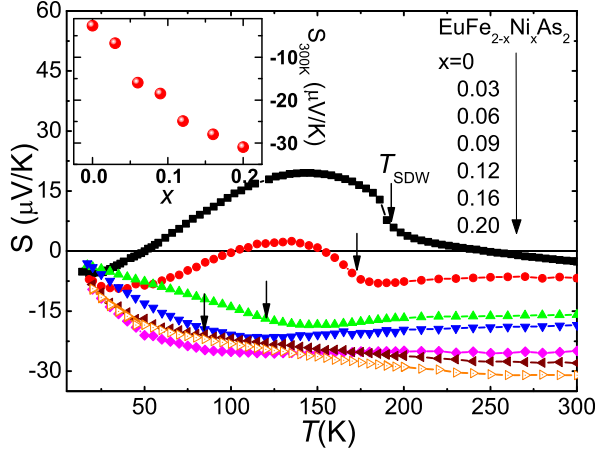


FIG. 3: (Color online) Temperature dependence of thermopower for the $\text{EuFe}_{2-x}\text{Ni}_x\text{As}_2$ samples. The inset shows the thermopower value at 300 K plotted as a function of Ni content x .

resembles that observed in $\text{BaFe}_{2-x}\text{Ni}_x\text{As}_2$ crystals.[23] With increasing Ni content x , T_{SDW} shifts to lower temperatures. For $x \geq 0.16$ the SDW transition is completely suppressed, however, no superconducting transition was observed down to the lowest temperature in the present study. Instead, two kinks in ρ at low temperatures are present, which can be seen more clearly in the derivative plots as shown in the inset of Fig. 2. It is probable that they share the same origin as that of undoped EuFe_2As_2 under magnetic fields, which is related to the different magnetic states of Eu^{2+} moments[33].

Figure 3 shows the temperature dependence of thermopower (S) for $\text{EuFe}_{2-x}\text{Ni}_x\text{As}_2$ samples. The sign reversal behavior, which manifests multi-band scenario, is observed for $x=0$ and 0.03. The value of S for the other samples is negative. With increasing Ni content, the room-temperature thermopower is pushed toward more negative values, as shown in the inset of Fig. 3. For a simple two-band model with electrons and holes, S can be expressed as,

$$S = \frac{n_h \mu_h |S_h| - n_e \mu_e |S_e|}{n_h \mu_h + n_e \mu_e}, \quad (1)$$

where $n_{h(e)}$, $\mu_{h(e)}$ and $|S_{h(e)}|$ denote the concentration, mobility and thermopower contribution of the holes(electrons), respectively. Therefore, the increase in $|S|$ suggests that Ni doping increases the electron concentration. Meanwhile, the anomaly due to the SDW transition is suppressed to lower temperatures and is no longer visible for $x=0.16$, in agreement with the above resistivity measurements. Recently, it was found that there exists enhanced thermopower in the superconducting window of $\text{SmFe}_{1-x}\text{Co}_x\text{AsO}$ system.[20] In the present system, no such enhancement was observed, which may be related to the absence of superconductivity.

Figure 4(a) shows the temperature dependence of mag-

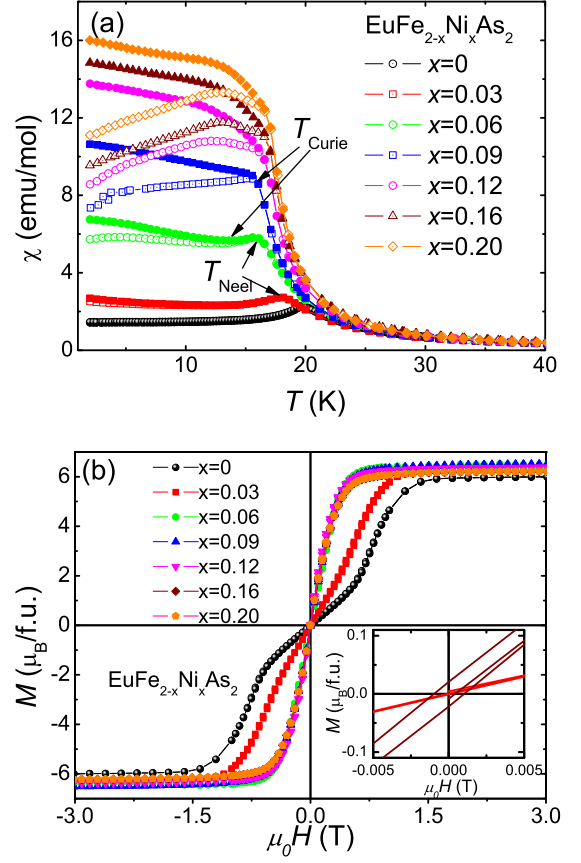


FIG. 4: (Color online) (a) Temperature dependence of zero-field cooling (ZFC) (open symbols) and field-cooling (FC) (solid symbols) magnetic susceptibility for the $\text{EuFe}_{2-x}\text{Ni}_x\text{As}_2$ samples. (b) Field dependence of magnetization at 2 K for the $\text{EuFe}_{2-x}\text{Ni}_x\text{As}_2$ samples. The inset shows an expanded plot of the low field region for $x=0.03$ and 0.16.

netic susceptibility (χ) for the $\text{EuFe}_{2-x}\text{Ni}_x\text{As}_2$ samples below 50 K under an applied field of 20 Oe. The χ data of $25 \text{ K} \leq T \leq 180 \text{ K}$ for $x \geq 0.03$ basically fall onto the same curve, which can be well fitted by the modified Curie-Weiss law,

$$\chi = \chi_0 + \frac{C}{T - \theta}, \quad (2)$$

where χ_0 denotes the temperature-independent term, C the Curie-Weiss constant and θ the paramagnetic Curie temperature. The refined parameters are $C = 8.0(1) \text{ emu-K/mol}$ and $\theta = 19(1) \text{ K}$. The calculated effective moment P_{eff} is $\sim 8 \mu_B$ per formula unit, close to the theoretical value of $7.94 \mu_B$ for a free Eu^{2+} ion. It is evident that the valence state of Eu ions remains +2 and ferromagnetic interaction between Eu^{2+} moments dominates up to 10% Ni doping. The anomaly in susceptibility due to the SDW transition is hardly observed even after subtracting the Curie-Weiss contribution of Eu^{2+} moments. On further cooling, a sharp peak can be observed in both

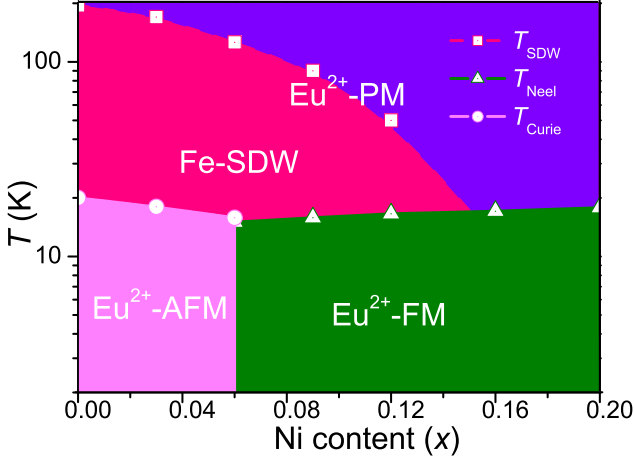


FIG. 5: (Color online) Magnetic phase diagram for $\text{EuFe}_{2-x}\text{Ni}_x\text{As}_2$ system ($0 \leq x \leq 0.2$).

χ_{ZFC} and χ_{FC} for $x=0.03$ at ~ 19 K, similar to that observed in undoped EuFe_2As_2 . [25] We ascribe this peak to the AFM ordering of Eu^{2+} moments. With increasing Ni content to 0.06, the peak shifts to ~ 16 K. Surprisingly, for the same sample, a small bifurcation between ZFC and FC curves develops below ~ 13 K, suggesting the formation of ferromagnetic domains. For $x \geq 0.09$, an obvious divergence between χ_{ZFC} and χ_{FC} is seen, suggesting the emergence of FM ordered state. It is also noted that there exists a broad peak below T_{Curie} in the ZFC curves for $x \geq 0.12$. Interestingly, T_{Curie} and T_{Peak} coincide with aforementioned two kinks in ρ at low temperatures, respectively. In EuFe_2As_2 single crystals, we have observed a metamagnetic phase with applied field perpendicular to the c -axis [33]. Thus we speculate that T_{Peak} may be related to a successive metamagnetic transition.

Figure 4(b) shows the field dependence of magnetization for the $\text{EuFe}_{2-x}\text{Ni}_x\text{As}_2$ samples at 2 K. For $x=0.03$, a slope change in the M - H curve can be seen clearly at $\mu_0 H = 0.55$ T, which is ascribed to a field-induced metamagnetic transition. [25, 33, 34] Moreover, there is no hysteresis loop in the low field region, consistent with the AFM ground state of Eu^{2+} moments. For the other samples, however, M increases steeply with initial increasing H . In addition, small hysteresis loops are observed. These results are in agreement with the above susceptibility measurements, suggesting that Eu^{2+} moments are FM ordered for $x \geq 0.06$. It is noted that all the saturated magnetic moments are around $6.3 \mu_B$ per formula, which is smaller than the theoretical value of $7 \mu_B$ for a free Eu^{2+} ion. This discrepancy is attributed to presence of impurity phases, whose magnetic response is much weaker.

Our experimental results on the physical properties of the $\text{EuFe}_{2-x}\text{Ni}_x\text{As}_2$ system are summarized in the magnetic phase diagram in Fig. 5. The parent compound

EuFe_2As_2 shows AFM ordering of Eu^{2+} moments at 20 K as well as SDW ordering of Fe moments at 195 K. With Ni doping, both the orderings are suppressed. On one hand, the SDW transition is gradually suppressed and eventually disappears at $x=0.16$. Nevertheless, no superconductivity was observed down to 2 K. On the other hand, the magnetic ordering of Eu^{2+} moments changes from AFM to FM at $x \approx 0.06$. This observation is surprising in view of the AFM ordering of Eu^{2+} moments in both the end members EuFe_2As_2 and EuNi_2As_2 [35]. By contrast, T_{Neel} remains nearly unchanged upon 10% Fe doping in EuNi_2As_2 . [36]

The AFM structure of Eu^{2+} moments in EuFe_2As_2 is proposed to be of A -type, *i.e.* FM coupling for intralayer Eu^{2+} moments while AFM coupling for interlayer Eu^{2+} moments. [25, 33, 34]. The distance between nearest Eu^{2+} layers is ~ 6 Å hence direct overlap of interlayer Eu $4f$ orbitals can be neglected. Therefore, the AFM exchange between interlayer Eu^{2+} moments is probably ascribed to the carrier-mediated Ruderman-Kittel-Kasuya-Yosida (RKKY) interaction. [35] The RKKY exchange coupling $J_{\text{RKKY}} \propto -\frac{\alpha \cos \alpha - \sin \alpha}{\alpha^4}$, where $\alpha = 2k_F R$, R denotes the distance between two magnetic moments and k_F the Fermi vector. One can see that J_{RKKY} oscillates between AFM (negative) and FM (positive) at the variation of $2k_F R$. Considering the dimensionality of the Fermi surfaces, it is probably that heavy 3-D hole pocket derived from Fe d_z states [18] is responsible for mediating the RKKY interaction. Substitution of Fe with Ni introduces electrons, which results in the decrease of k_F . Meanwhile, R is also shortened, as indicated by the reduction of c -axis. Thus the interlayer coupling may be tuned from AFM to FM. On the other hand, the FM interaction within the Eu^{2+} layers persists up to 10% Ni doping. As a consequence, a FM ordering of Eu^{2+} moments is established. In contrast, the dominant interaction between Eu^{2+} moments in EuNi_2As_2 is antiferromagnetic, as indicated by negative paramagnetic Curie temperature [35]. This may account for the robust AFM ordering of Eu^{2+} moments upon Fe doping in EuNi_2As_2 . The clarification of these issues relies on further ARPES as well as neutron diffraction studies.

In the iron-based arsenides, superconductivity generally emerges as the SDW order is suppressed by the carrier doping. As a matter of fact, superconductivity with the maximum T_c of ~ 20 K has been observed in $\text{BaFe}_{2-x}\text{Ni}_x\text{As}_2$ system. [23] Thus, the absence of superconductivity in $\text{EuFe}_{2-x}\text{Ni}_x\text{As}_2$ may be relevant to the magnetism of Eu^{2+} ions. The RKKY interaction mentioned above may hinder the Cooper pairing for superconductivity. Recently, re-entrant superconducting behavior has been observed in a high pressure study of EuFe_2As_2 crystal. [37] The results suggest that once T_c becomes smaller than the magnetic ordering temperature of Eu^{2+} moments, superconductivity will be completely suppressed. If $\text{EuFe}_{2-x}\text{Ni}_x\text{As}_2$ were superconducting, its maximum T_c would be ~ 6 K smaller than that of $\text{BaFe}_{2-x}\text{Ni}_x\text{As}_2$ due to the existence of paramag-

netic Eu^{2+} ions[37]. The assumed T_c is below the Curie temperatures. This could account for the absence of superconductivity in $\text{EuFe}_{2-x}\text{Ni}_x\text{As}_2$ system.

IV. CONCLUSION

In summary, we have systematically studied the transport and magnetic properties on a series of $\text{EuFe}_{2-x}\text{Ni}_x\text{As}_2$ polycrystalline samples with $0 \leq x \leq 0.2$. It is found that both the SDW transition associated with the Fe moments and the AFM ordering of Eu^{2+} moments are suppressed upon Ni doping. Though the SDW transition is completely suppressed for $x \geq 0.16$, no superconducting transition is observed down to 2 K. Surprisingly,

a FM ground state of Eu^{2+} moments emerges for $x \geq 0.06$. A detailed magnetic phase diagram is presented and discussed within the RKKY framework. Our results suggest there exists a strong coupling the magnetism of Eu^{2+} ions and the electronic state in the $[\text{Fe}_{2-x}\text{Ni}_x\text{As}_2]^{2-}$ layers.

Acknowledgments

We would like to thank J. H. Dai and Q. Si for helpful discussions. This work is supported by the National Basic Research Program of China (No.2006CB601003 and 2007CB925001) and the PCSIRT of the Ministry of Education of China (IRT0754).

-
- [1] Y. Kamihara, T. Watanabe, M. Hirano, and H. Hosono, *J. Am. Chem. Soc.* **130**, 3296 (2008).
 - [2] X. H. Chen, T. Wu, G. Wu, R. H. Liu, H. Chen, and D. F. Fang, *Nature* **453**, 761 (2008).
 - [3] G. F. Chen, Z. Li, D. Wu, G. Li, W. Z. Hu, J. Dong, P. Zheng, J. L. Luo, and N. L. Wang, *Phys. Rev. Lett.* **100**, 247002 (2008).
 - [4] Z. A. Ren, J. Yang, W. Lu, W. Yi, G. C. Che, X. L. Dong, L. L. Sun, and Z. X. Zhao, *Materials Research Innovations* **12**, 105 (2008).
 - [5] Z. A. Ren, J. Yang, W. Lu, W. Yi, X. L. Shen, Z. C. Li, G. C. Che, X. L. Dong, L. L. Sun, F. Zhou, and Z. X. Zhao, *Europhysics Lett.* **82**, 57002 (2008).
 - [6] H. H. Wen, G. Mu, L. Fang, H. Yang, and X. Y. Zhu, *Europhysics Lett.* **82**, 17009 (2008).
 - [7] C. Wang, L. J. Li, S. Chi, Z. W. Zhu, Z. Ren, Y. K. Li, Y. T. Wang, X. Lin, Y. K. Luo, S. Jiang, X. F. Xu, G. H. Cao, and Z. A. Xu, *Europhysics Lett.* **83**, 67006 (2008).
 - [8] V. Johnson and W. Jeitschko, *J. Solid State Chem.* **11**, 161 (1974).
 - [9] P. Quebe, L. J. Terbuchte, and W. Jeitschko, *Journal of Alloys and Compounds* **302**, 70(2000).
 - [10] M. Pfisterer, and G. Nagorsen, *Z. Naturforsch. B: Chem. Sci.* **35**, 703 (1980).
 - [11] M. Pfisterer, and G. Nagorsen, *Z. Naturforsch. B: Chem. Sci.* **38**, 811 (1983).
 - [12] R. Marchand, W. Jeitschko, *J. Solid State Chem.* **24**, 351 (1978).
 - [13] G. Wu, H. Chen, T. Wu, Y. L. Xie, Y. J. Yan, R. H. Liu, X. F. Wang, J. J. Ying, and X. H. Chen, *J. Phys.: Condens. Matter* **20**, 422201 (2008).
 - [14] M. Rotter, M. Tegel, D. Johrendt, I. Schellenberg, W. Hermes, and R. Pöttgen, *Phys. Rev. B* **78**, 020503(R) (2008).
 - [15] C. de la Cruz, Q. Huang, J. W. Lynn, J. Li, W. Ratcliff II, H. A. Mook, G. F. Chen, J. L. Luo, N. L. Wang, and Pengcheng Dai, *Nature* **453**, 899 (2008).
 - [16] K. Haule, J. H. Shim, and G. Kotliar, *Phys. Rev. Lett.* **100**, 226402 (2008).
 - [17] C. Cao, P. J. Hirschfeld, and H. P. Cheng, *Phys. Rev. B* **77**, 220506(R) (2008).
 - [18] D. J. Singh, and M. H. Du, *Phys. Rev. Lett.* **100**, 237003 (2008).
 - [19] A. S. Sefat, A. Huq, M. A. McGuire, R. Jin, B. C. Sales, D. Mandrus, L. M. D. Cranswick, P. W. Stephens, and K. H. Stone, *Phys. Rev. B* **78**, 104505 (2008).
 - [20] C. Wang, Y. K. Li, Z. W. Zhu, S. Jiang, X. Lin, Y. K. Luo, S. Chi, L. J. Li, Z. Ren, M. He, H. Chen, Y. T. Wang, Q. Tao, G. H. Cao, and Z. A. Xu, *Phys. Rev. B* **79**, 054521 (2009).
 - [21] G. H. Cao, S. Jiang, X. Lin, C. Wang, Y. K. Li, Z. Ren, Q. Tao, J. H. Dai, Z. A. Xu, and F. C. Zhang, *arXiv:0807.4328*.
 - [22] A. S. Sefat, R. Jin, M. A. McGuire, B. C. Sales, D. J. Singh, and D. Mandrus, *Phys. Rev. Lett.* **101**, 117004 (2008).
 - [23] L. J. Li, Y. K. Luo, Q. B. Wang, H. Chen, Z. Ren, Q. Tao, Y. K. Li, X. Lin, M. He, Z. W. Zhu, G. H. Cao, and Z. A. Xu, *New J. Phys.*, *in press*.
 - [24] A. Leithe-Jasper, W. Schnelle, C. Geibel, and H. Rosner, *Phys. Rev. Lett.* **101**, 207004 (2008).
 - [25] Z. Ren, Z. W. Zhu, S. Jiang, X. F. Xu, Q. Tao, C. Wang, C. M. Feng, G. H. Cao, and Z. A. Xu, *Phys. Rev. B* **78**, 052501 (2008).
 - [26] H. S. Jeevan, Z. Hossain, D. Kasinathan, H. Rosner, C. Geibel, and P. Gegenwart, *Phys. Rev. B*, **78**, 052502 (2008).
 - [27] M. Rotter, M. Tegel, and D. Johrendt, *Phys. Rev. Lett.* **101**, 107006 (2008).
 - [28] G. F. Chen, Z. Li, G. Li, W. Z. Hu, J. Dong, X. D. Zhang, P. Zheng, N. L. Wang, and J. L. Luo, *Chin. Phys. Lett.* **25**, 3403 (2008).
 - [29] K. Sasmal, B. Lv, B. Lorenz, A. M. Guloy, F. Chen, Y. Y. Xue, C. W. Chu, and *Phys. Rev. Lett.* **101**, 107007 (2008).
 - [30] H. S. Jeevan, Z. Hossain, D. Kasinathan, H. Rosner, C. Geibel, and P. Gegenwart, *Phys. Rev. B*, **78**, 092406 (2008).
 - [31] Y. P. Qi, Z. S. Gao, L. Wang, D. L. Wang, X. P. Zhang, and Y. W. Ma, *New J. Phys.*, *in press*.
 - [32] F. Izumi, and T. Ikeda, *Mater. Sci. Forum*, **198**, 321 (2000).
 - [33] S. Jiang, Y. K. Luo, Z. Ren, Z. W. Zhu, C. Wang, X. F. Xu, Q. Tao, G. H. Cao, and Z. A. Xu, *New J. Phys.*, *in press*.
 - [34] T. Wu, G. Wu, H. Chen, Y. L. Xie, R. H. Liu, X. F.

- Wang, and X. H. Chen, arXiv:0808.2247.
- [35] H. Raffius, E. Mörsen, B. D. Mosel, W. Müller-Warmuth, W. Jeitschko, L. Terbüchte, and T. Vomhof, J. Phys. Chem. Solids **54**, 135 (1993).
- [36] Z. Ren *et al.*, unpublished results.
- [37] C. F. Miclea, M. Nicklas, H. S. Jeevan, D. Kasinathan, Z. Hossain, H. Rosner, P. Gegenwart, C. Geibel, and F. Steglich, arXiv:0808.2026.